The Journal of Immunology

RESEARCH ARTICLE | FEBRUARY 15 2022

# Turnover of Murine Cytomegalovirus–Expanded CD8+ T Cells Is Similar to That of Memory Phenotype T Cells and Independent of the Magnitude of the Response FREE

Mariona Baliu-Piqué; ... et. al

*J Immunol* (2022) 208 (4): 799–806.
https://doi.org/10.4049/jimmunol.2100883

# Turnover of Murine Cytomegalovirus–Expanded CD8$^+$ T Cells Is Similar to That of Memory Phenotype T Cells and Independent of the Magnitude of the Response

**Mariona Baliu-Piqué,*[,1,2] Julia Drylewicz,*[,1] Xiaoyan Zheng,[†,1] Lisa Borkner,[†] Arpit C. Swain,[‡] Sigrid A. Otto,* Rob J. de Boer,[‡] Kiki Tesselaar,*[,3] Luka Cicin-Sain,[†,§,3] and José A. M. Borghans*[,3]**

**The potential of memory T cells to provide protection against reinfection is beyond question. Yet, it remains debated whether long-term T cell memory is due to long-lived memory cells. There is ample evidence that blood-derived memory phenotype CD8$^+$ T cells maintain themselves through cell division, rather than through longevity of individual cells. It has recently been proposed, however, that there may be heterogeneity in the lifespans of memory T cells, depending on factors such as exposure to cognate Ag. CMV infection induces not only conventional, contracting T cell responses, but also inflationary CD8$^+$ T cell responses, which are maintained at unusually high numbers, and are even thought to continue to expand over time. It has been proposed that such inflating T cell responses result from the accumulation of relatively long-lived CMV-specific memory CD8$^+$ T cells. Using in vivo deuterium labeling and mathematical modeling, we found that the average production rates and expected lifespans of mouse CMV-specific CD8$^+$ T cells are very similar to those of bulk memory-phenotype CD8$^+$ T cells. Even CMV-specific inflationary CD8$^+$ T cell responses that differ 3-fold in size were found to turn over at similar rates.** ***The Journal of Immunology*****, 2022, 208: 799–806.**

Memory CD8$^+$ T cells are a crucial component of the adaptive immune response to viruses. Ag-specific memory CD8$^+$ T cells convey immune protection against viral infections that may last for long periods of time, sometimes even lifelong. There is ample evidence that memory T cells isolated from the blood and lymph nodes are relatively short-lived. Their lifespan is much shorter than that of naive T ($T_N$) cells, and far shorter than the long-term immune protection they convey (1–10). Memory T cell populations are heterogeneous, both phenotypically and functionally. They consist of phenotypically defined subpopulations, such as central memory T ($T_{CM}$) and effector memory T ($T_{EM}$) cells, and of subsets that differ in terms of exposure to their cognate Ag. In vivo deuterium labeling studies have shown that different subsets of memory T cells can have different kinetics. CD4$^+$ $T_{EM}$ cells were shown to have shorter lifespans than did $T_{CM}$ cells (10), and yellow fever virus (YFV)–specific memory T cells generated by vaccination, which can persist for years, were found to have longer lifespans than did bulk memory-phenotype cells (11).

CMV infection is a persistent, chronic infection, which, in contrast to YFV vaccination, results in continual Ag presentation. CMV is under constant immune surveillance, and it triggers ongoing CD8$^+$ T cell responses that provide effective viral control for long periods of time. A hallmark of the CD8$^+$ T cell response to CMV infection is the steady maintenance or accumulation of large populations of virus-specific effector CD8$^+$ T cells over time, a phenomenon termed memory inflation (12). Expanded CD8$^+$ T cell populations specific for unique CMV epitopes can become extraordinarily large, composing up to 20% of the total memory T ($T_M$) CD8$^+$ cell pool (13–18). These large CMV-specific T cell responses turned out to be maintained dynamically, through continuous production of relatively short-lived cells (19). Nevertheless, a face-to-face comparison of the in vivo dynamics of CMV-specific and bulk memory-phenotype CD8$^+$ T cells suggested that inflating CMV-specific memory CD8$^+$ T cell responses are composed of cells that are longer-lived than other memory cells. This has led to the hypothesis that T cell inflation arises from the accumulation of relatively long-lived CMV-specific memory T cells (20).

In this study, we addressed this hypothesis using in vivo deuterium labeling and mathematical modeling, the state-of-the-art techniques to quantify lymphocyte turnover, in the setting of murine

*Center for Translational Immunology, University Medical Center Utrecht, Utrecht, the Netherlands; [†]Department of Viral Immunology, Helmholtz Centre for Infection Research, Braunschweig, Germany; [‡]Theoretical Biology, Utrecht University, Utrecht, The Netherlands; and [§]German Center for Infection Research, Partner Site, Hannover-Braunschweig, Germany

Received for publication September 9, 2021. Accepted for publication December 8, 2021.

[1]M.B.-P., J.D., and X.Z. contributed equally to this work.

[2]Current address: Immunotherapy Manufacturing Center, Galaria-Sergas, Santiago de Compostela, Spain.

[3]K.T., L.C.-S., and J.A.M.B. are cosenior authors.

ORCIDs: 0000-0002-9276-8839 (M.B.-P); 0000-0002-9434-8459 (J.D.); 0000-0001-9091-1630 (X.Z.); 0000-0001-5718-649X (L.B.); 0000-0002-7816-1053 (A.C.S.); 0000-0002-2130-691X (R.J.d.B.); 0000-0002-9847-0814 (K.T.); 0000-0003-3978-778X (L.C.-S.); 0000-0002-2931-0390 (J.A.M.B.).

This work was supported by funding from the European Union Seventh Framework Programme (FP7/2007–2013) through the Marie-Curie Action "Quantitative T Cell Immunology" Initial Training Network, with reference FP7-PEOPLE-2012-ITN 317040-QuanTI supporting M.B.-P., and European Research Council Grant 260934 to L.C.-S.. X.Z. was supported by a Chinese Scientific Council scholarship. A.C.S. was supported by Netherlands Organisation for Scientific Research Grant ALWOP.265.

Address correspondence and reprint requests to Prof. José A.M. Borghans, University Medical Center Utrecht, PO Box 85090, 3508 AB, Utrecht, the Netherlands. E-mail address: j.borghans@umcutrecht.nl

The online version of this article contains supplemental material.

Abbreviations used in this article: CI, confidence interval; dpi, day postinfection; GC/MS, gas chromatography/mass spectrometry; KNL, KCSRNRQYL; MCMV, murine CMV; SL, SSIEFARL; 129/Sv, 129S2/SvPas Crl; $T_{CM}$, central memory T; $T_{EM}$, effector memory T; Tet$^+$, tetramer-positive; $T_M$, total memory T; $T_N$, naive T; YFV, yellow fever virus.

CMV (MCMV) infection, a relevant experimental model to study memory T cell inflation (14). In contrast to the postulated hypothesis that CMV-specific T cells may have extended lifespans, we found no significant difference in the expected lifespans of MCMV-specific CD8$^+$ T cells and bulk memory-phenotype CD8$^+$ T cells. Using recombinant viruses inducing inflationary CD8$^+$ T cell responses of different magnitudes, we found that MCMV-specific T cells composing small and large inflationary T cell responses had very similar turnover rates.

## Materials and Methods

### *Mice*

129S2/SvPas Crl (129/Sv) mice were purchased from Charles River Laboratories (Sulzfeld, Germany). Mice were housed and handled in accordance with good animal practice as defined by the Federation of Laboratory Animal Science Associations and the national animal welfare body Die Gesellschaft für Versuchstierkunde (Society of Laboratory Animal Science). All animal experiments were approved by the responsible state office (Lower Saxony State Office of Consumer Protection and Food Safety, Germany; permit number 33.19-42502-04-15/1836 and by the Animal Experiments Committee of Utrecht University, IVD Utrecht, the Netherlands; DEC AVD115002016714).

### *Viruses*

Bacterial artificial chromosome–derived recombinant viruses MCMV$^{ie2SL}$ and MCMV$^{M45SL}$ were generated and propagated as described previously (18), and the recombinant virus MCMV$^{ie2KNL}$ was generated and propagated as described in Borkner et al. (21).

### *In vivo infection*

Female 8-wk-old mice were infected with $2 \times 10^5$ PFU of MCMV$^{ie2SL}$ ($n = 40$), MCMV$^{M45SL}$ ($n = 37$), or MCMV$^{ie2KNL}$ ($n = 41$) and housed in specific pathogen-free conditions throughout the experiment. Noninfected sex- and age-matched mice were used as controls ($n = 10$).

### *Stable isotope labeling*

One hundred twenty days after MCMV infection, mice received 8% deuterated water (99.8% $^2H_2O$, Cambridge Isotope Laboratories) in their drinking water for 28 days. At day 4, mice were given an i.p. boost injection of 15 ml/kg $^2H_2O$ in PBS. To determine deuterium enrichment in the body water, EDTA plasma was collected during the up- and down-labeling phase and was frozen and stored at −80°C until analysis.

### *Sampling and cell preparation*

Spleen, thymus, and blood were isolated at different time points during and after label administration. Blood was collected in EDTA tubes. Single-cell suspensions from blood, spleen, and thymus were obtained as described previously (22).

### *Flow cytometry and cell sorting*

To determine the fraction of SSIEFARL (SL) and KCSRNRQYL (KNL) epitope-specific T cells, single-cell suspensions from blood and spleen were stained with allophycocyanin-conjugated SL-K$^b$ or KNL-D$^b$ tetramers for 15 min at 4°C. Samples were further stained for 30 min at 4°C with anti–CD3-allophycocyanin-eFluor 780 (clone 17A2; eBioscience), anti–CD3e-FITC (clone 145-2C11; BD Phamingen), anti-CD3-V500 (clone 500A2; BD), anti–CD4-Pacific Blue (clone GK1.5; BioLegend), anti–CD4-Brilliant Violet 650 (clone GK1.5; BD Horizon), anti–CD4-allophycocyanin-H7 (GK1.5; BD), anti–CD8a-PerCP/Cy5.5 (clone 53-6.7; BioLegend), anti–CD8a-Brillian Violet 786 (clone 53-6.7; BD), anti–CD44-Alexa Fluor 700 (clone IM7; BioLegend), anti–CD44-Alexa Fluor 450 (IM7; eBioscience), anti–CD62L-eVolve 605 (clone MEL-14; eBioscience), anti–CD62L-FITC (MEL-14; eBioscience), and anti–CD127-PE/Cy7 (clone A7R34; BioLegend) mAbs. For intracellular staining, cells were subsequently fixed for 20 min at room temperature with 100 μl of fixation/permeabilization buffer of the FoxP3 Transcription Factor Staining Set (eBioscience), permeabilized for 15 min at room temperature in 100 μl of permeabilization buffer (eBioscience), and stained with Ki-67-PE (clone 16A8; BioLegend) in 100 μl of permeabilization buffer for 30 min at room temperature. Cells were analyzed on an LSRFortessa flow cytometer using FACSDiva software (BD Biosciences) and FlowJo software (version 9.8.3). For infected mice, tetramer-positive (Tet$^+$) (CD3$^+$CD8$^+$Tet$^+$) T cells and tetramer-negative $T_N$ (CD3$^+$CD8$^+$Tet$^-$CD62L$^+$CD44$^-$), $T_{CM}$ (CD3$^+$CD8$^+$Tet$^-$CD62L$^+$CD44$^+$), and $T_{EM}$ (CD3$^+$CD8$^+$Tet$^-$CD62L$^-$CD44$^+$) cells were sorted from spleen on a FACSAria II SORP (BD Biosciences), FACSAria III (BD Biosciences), or MoFlo XDP cell sorter (Supplemental Fig. 1A). For uninfected mice, $T_N$, $T_{CM}$, and $T_{EM}$ cells were sorted from spleen on a FACSAria III (BD Biosciences).

### *DNA isolation*

Genomic DNA was isolated from total thymocytes and from sorted T cell subsets from MCMV-infected and uninfected mice according to the manufacturer's instructions using the NucleoSpin Blood QuickPure kit (Macherey-Nagel), and stored at −20°C until further analysis.

### *Measurement of $^2H_2O$ enrichment in body water and DNA*

Deuterium enrichment in plasma and DNA was analyzed by gas chromatography/mass spectrometry (GC/MS) using an Agilent 5973/6890 GC/MS system (Agilent Technologies). Plasma was derivatized to acetylene ($C_2H_2$) as previously described (5). The derivative was injected into the GC/MS system equipped with a PoraPLOT Q 25 × 0.32 column (Varian) and measured in selected ion monitoring mode monitoring ions $m/z$ 26 (M+0) and $m/z$ 27 (M+1). From the ratio of ions, plasma deuterium enrichment was calculated by calibration against standard samples of known enrichment. DNA obtained from sorted lymphocytes and granulocytes was hydrolyzed to deoxyribonucleotides and derivatized to pentafluoro tri-acetate (5). The derivative was injected into the GC/MS system equipped with a DB-17 column (Agilent Technologies) and measured in selected ion monitoring mode monitoring ions $m/z$ 435 (M+0) and $m/z$ 436 (M+1). From the ratio of ions, we calculated DNA deuterium enrichment by calibration against deoxyadenosine standards of known enrichment, as previously described (23).

### *Mathematical modeling of T cell dynamics*

We deduced the dynamics of tetramer-negative $T_N$, tetramer-negative $T_{CM}$, tetramer-negative $T_{EM}$, and tetramer-negative $T_M$ (calculated as the weighted average of $T_{CM}$ and $T_{EM}$ cells) CD8$^+$ cells, and of Tet$^+$ CD8$^+$ T cells from the deuterium labeling data using previously published mathematical models (3, 24). In brief, to monitor the changing levels of deuterium in body water during the course of the experiment, a simple label enrichment/decay curve was fitted to the deuterium enrichment in plasma (3):

$$S(t) = \begin{cases} f(1 - e^{-\delta t}) + S_0 e^{-\delta t}, t \le \tau \\ \left[f(1 - e^{-\delta \tau}) + S_0 e^{-\delta \tau}\right] e^{-\delta (t-\tau)}, t > \tau \end{cases} \quad (1)$$

where $S(t)$ is the fraction of deuterium in plasma at time $t$ (in days), $f$ is the predicted plateau value of deuterium enrichment in the plasma, $\delta$ is the turnover rate of body water per day, $S_0$ is the plasma enrichment level attained due to the i.p. $^2H_2O$ boost, and $^2H_2O$ administration was stopped at $\tau = 28$ days. The level of label incorporation in the different cell subsets was described by

$$\frac{dl(t)}{dt} = pcS(t) - d^* l(t). \quad (2)$$

Here, $l(t)$ is the fraction of labeled DNA in the cell subset, $p$ is the average (per capita) production rate of the cells, $d^*$ is the average (per capita) rate at which labeled cells are lost [which need not be equal to the average loss rate of cells in the population (24)], and $c$ is an amplification factor, which accounts for the multiple hydrogen atoms that can be replaced by deuterium (see Ref. 3). To estimate the value of $c$, we first fitted Eq. 2 for a kinetically homogeneous population ($p = d^*$) (5) to the level of deuterium enrichment in the DNA of total thymocytes, as they are known to have a high turnover rate (5). The resulting estimated value of $c$ was subsequently fixed to estimate the turnover rates of $T_N$, $T_{CM}$, $T_{EM}$, and $T_M$ cells and Tet$^+$ CD8$^+$ T cells. The best fits to the plasma and thymocyte data are shown in Supplemental Fig. 2 (see Supplemental Table I for the estimated parameter values). When modeling the deuterium enrichment levels of $T_N$ cells, a time delay ($\Delta$) was introduced between T cell production in the thymus and the appearance of labeled DNA in $T_N$ cells in the spleen, based on previous observations (5). This was done by incorporating a delayed labeling curve of the deuterium enrichment in plasma [i.e., $S(t - \Delta)$] in Eq. 2 when fitting the dynamics of $T_N$ cells.

To estimate the rate of change in cell numbers, $r$, in the $T_N$, $T_{CM}$, $T_{EM}$, $T_M$, and Tet$^+$ T cell populations, we used a simple exponential growth/decay model, $\frac{dN(t)}{dt} = rN(t) = (p - d)N(t)$, which we fitted to the cell number data from the start of the experiment [i.e., 120 days postinfection (dpi)] until 550 days later (see Table II and Supplemental Fig. 3). Results were very similar when $r$ was estimated based on cell numbers during the first 140 days of the experiment. Based on the resulting value of $r$ and the estimated value of $p$ from Eq. 2, the cellular loss rates, $p - r$, were calculated (see Table II). The expected lifespans of cells can be calculated as the inverse of their average loss rates, that is, as $1/d$.

Best fits to the labeling and cell number data were determined by minimizing the sum of squared residuals using the R function modCost() of the FME package (25). The fractions of labeled DNA, x, were transformed using the function arcsin(sqrt(x)) before the fitting procedure. Fitting the cell number data yielded estimates for the initial cell number at the start of the experiment at 120 dpi, $N(0)$, and the exponential growth rate, $r$. The 95% confidence intervals (CIs) on the estimated parameters for both labeling and cell number data were determined using a bootstrap method where the data points were resampled 500 times. Fitting the exponential growth/decay model to these 500 data samples yielded 500 bootstrap trajectories. The 95% CI trajectories for the cell numbers were calculated by taking the 95% CI of these 500 bootstraps at each time point.

### *Statistical analysis*

Statistical analyses were performed using GraphPad Prism. Comparisons between two and more groups were performed using Kruskal–Wallis and Dunn's multiple comparison tests. A $p$-value $<0.05$ was considered significant.

## Results

### *Induction of inflationary CD8$^+$ T cell responses of different magnitude and phenotype*

To study the kinetics of MCMV-specific and inflationary CD8$^+$ T cell responses during the memory phase of MCMV infection, we made use of 129/Sv mice to benefit from the well-defined $H^{2b}$ MHC class I haplotype and the well-characterized arrays of epitopes associated with it, while circumventing a protective dominant role of NK cells in controlling the infection (18, 26). The avidity of the viral epitope together with its context of gene expression define the kinetics and magnitude of the cognate inflationary CD8$^+$ T cell response (18). We used three well-characterized MCMV mutants expressing low-avidity or high-avidity epitopes in different genetic contexts: the recombinant MCMV$^{ie2SL}$, which expresses the high-avidity HSV-1 epitope SL inserted at the C terminus of the immediate-early 2 (*ie2*) gene (18); the MCMV$^{ie2KNL}$ mutant expressing the low-avidity epitope KNL also inserted at the C terminus of the *ie2* gene (21); and the MCMV$^{m45SL}$ recombinant, which expresses the same epitope as MCMV$^{ie2SL}$ inserted in a different genetic context, the early *m45* gene (18).

SL-specific and KNL-specific CD8$^+$ T cells were analyzed 120 dpi using tetramer staining to determine the magnitude and the phenotype of the inflating T cell response. As previously described (21), the SL and the KNL epitopes expressed within the *ie2* gene induced larger inflationary T cell responses than does the SL epitope expressed within the *m45* gene (Fig. 1A). MCMV$^{ie2SL}$ induced the inflationary response of the highest magnitude; a median of 13% of total CD8$^+$ T cells were SL Tet$^+$. The size of the specific response to MCMV$^{ie2KNL}$ was ~9% of the CD8$^+$ T cell pool, and significantly larger than the response to MCMV$^{m45SL}$, which remained below 5%. Yet, even the latter recombinant virus induced a clearly detectable Tet$^+$ CD8$^+$ T cell population (Fig. 1A).

Ag-specific CD8$^+$ T cells composing an inflationary response typically present an effector phenotype and maintain their effector function (14). Accordingly, the vast majority (>80%) of Tet$^+$ CD8$^+$ T cells composing large inflationary responses (MCMV$^{ie2SL}$ and MCMV$^{ie2KNL}$) had a $T_{EM}$ cell phenotype (CD44$^+$CD62L$^-$). In contrast, only 60% of the Tet$^+$ CD8$^+$ T cells induced by MCMV$^{m45SL}$ presented a $T_{EM}$ cell phenotype, whereas the remaining 40% expressed $T_{CM}$ cell markers (CD44$^+$CD62L$^+$) (Fig. 1B, Supplemental Fig. 1B, 1C). Less than 2% of the Tet$^+$ T cells had a $T_N$ cell phenotype (CD44$^-$CD62L$^+$).

### *Ki-67 expression pattern of CD8$^+$ T cells does not differ between MCMV-induced inflationary responses of different magnitude*

To study the dynamics of CD8$^+$ T cells in the stable phase of chronic MCMV infection, we first determined cell proliferation by measuring Ki-67 expression. The fraction of Ki-67$^{hi}$ cells within $T_N$, $T_{CM}$, and $T_{EM}$ CD8$^+$ cells was not significantly different between uninfected mice and chronically infected mice for all three viruses (Fig. 2). In line with previous reports (27), we found that the percentage of Ki-67$^{hi}$ cells was the lowest within $T_N$ cells (median over all groups of 0.4%), intermediate within $T_{CM}$ cells (median of 4.5%), and the highest within $T_{EM}$ cells (median of 12%) (Fig. 2B). Approximately 5% of the Tet$^+$ CD8$^+$ T cells were Ki-67$^{hi}$. For each viral infection, the total fraction of Ki-67$^{hi}$ cells within the Tet$^+$ cells was not significantly different from that of memory phenotype T cells, and it was in fact between the Ki-67 expression levels of $T_{EM}$ and $T_{CM}$ cells (Fig. 2B). Based on Ki-67 expression, we thus found no indication that inflated MCMV-specific CD8$^+$ T cells have different proliferation rates than do bulk memory phenotype CD8$^+$ T cells. Because Ki-67 only provides a snapshot marker of T

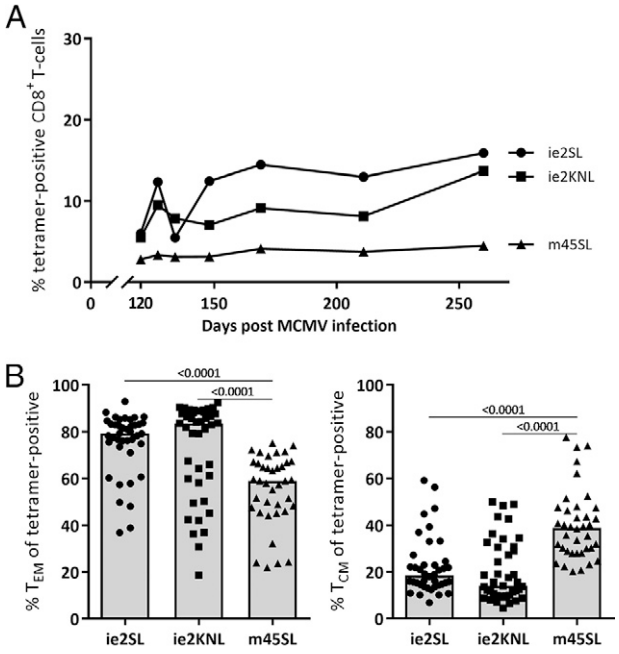


**FIGURE 1.** Recombinant viruses induce inflationary responses of different magnitude and phenotype. Mice (129/Sv) were infected with MCMV$^{ie2SL}$, MCMV$^{ie2KNL}$, or MCMV$^{m45SL}$, and at 120 dpi Tet$^+$ CD8$^+$ T cells from spleen were characterized. (**A**) Median percentage of Tet$^+$ cells within CD8$^+$ T cells over time ($n$ = 4–7 per time point per group). For significance, $p$-value = 0.04 for pooled time points of MCMV$^{ie2SL}$ versus MCMV$^{ie2KNL}$, $p$-value < 0.0001 for pooled time points of MCMV$^{ie2SL}$ versus MCMV$^{m45SL}$, and $p$-value = 0.0006 for pooled time points of MCMV$^{ie2KNL}$ versus MCMV$^{m45SL}$. Pooled samples of different time points were compared using Kruskal–Wallis and Dunn's multiple comparisons test. Data are pooled from two independent experiments. (**B**) Percentage of $T_{EM}$ (left; CD44$^+$CD62L$^-$) and $T_{CM}$ (right; CD44$^+$CD62L$^+$) cells within the Tet$^+$ CD8$^+$ T cell pool (MCMV$^{ie2SL}$ $n$ = 39, MCMV$^{ie2KNL}$ $n$ = 41, MCMV$^{m45SL}$ $n$ = 38). Data are pooled from two independent experiments. Bars represent the median percentage. For the % of $T_{EM}$ cells, $p$-value > 0.999 for pooled time points of MCMV$^{ie2SL}$ versus MCMV$^{ie2KNL}$, $p$-value < 0.0001 for pooled time points of MCMV$^{ie2SL}$ versus MCMV$^{m45SL}$, and $p$-value < 0.0001 for pooled time points of MCMV$^{ie2KNL}$ versus MCMV$^{m45SL}$. For the % of $T_{CM}$ cells, $p$-value = 0.976 for pooled time points of MCMV$^{ie2SL}$ versus MCMV$^{ie2KNL}$, $p$-value < 0.0001 for pooled time points of MCMV$^{ie2SL}$ versus MCMV$^{m45SL}$, and $p$-value < 0.0001 for pooled time points of MCMV$^{ie2KNL}$ versus MCMV$^{m45SL}$. Pooled samples of different time points were compared using Kruskal–Wallis and Dunn's multiple comparison tests. Median percentages of $T_N$, $T_{CM}$, and $T_{EM}$ cells within tetramer-negative and Tet$^+$ CD8$^+$ T cells in MCMV-infected and uninfected mice are shown in Supplemental Fig. 1B. Changes in the median percentage of $T_N$, $T_{CM}$, and $T_{EM}$ CD8$^+$ cells over time are shown in Supplemental Fig. 1C.

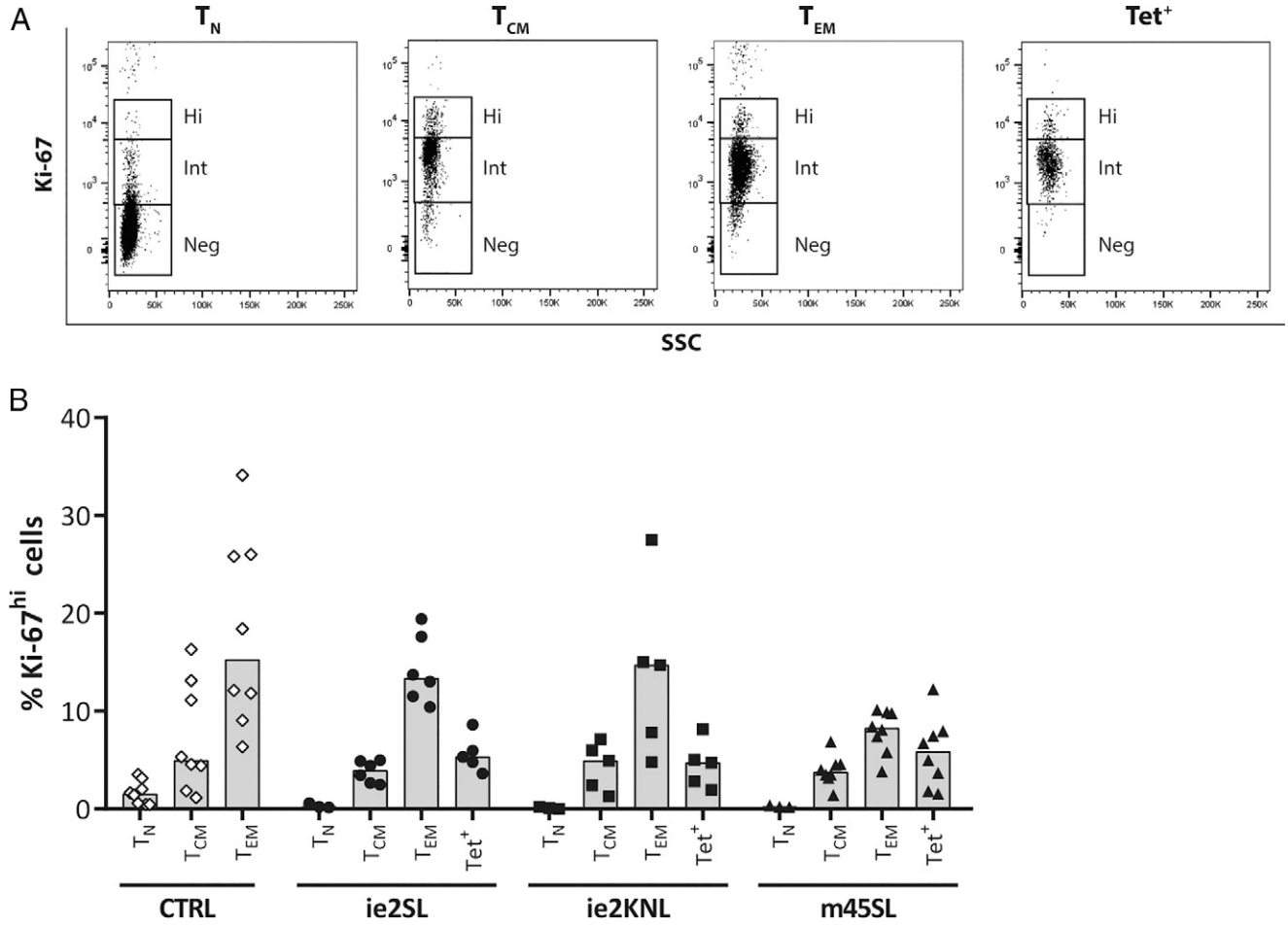


**FIGURE 2.** Percentage Ki-67$^{hi}$ cells within CD8$^+$ T cell subsets in MCMV-infected and uninfected mice. (**A**) Representative Ki-67 staining of $T_N$, $T_{CM}$, and $T_{EM}$ cells and Tet$^+$ CD8$^+$ T cells from blood of an MCMV$^{m45SL}$-infected mouse at 17 mo postinfection. (**B**) Fraction of Ki-67$^{hi}$ $T_N$, $T_{CM}$, and $T_{EM}$ cells and Tet$^+$ CD8$^+$ T cells from blood of MCMV$^{ie2SL}$-infected ($n$ = 4–6), MCMV$^{ie2KNL}$-infected ($n$ = 4–5), and MCMV$^{m45SL}$-infected ($n$ = 4–8) mice and age-matched and sex-matched uninfected mice (CTRL, $n$ = 8). For MCMV$^{ieKNL}$, $p$-value = 0.418 for pooled time points of % Ki-67$^{hi}$ Tet$^+$ versus $T_{EM}$ cells, $p$-value > 0.999 for pooled time points of % Ki-67$^{hi}$ Tet$^+$ versus $T_{CM}$ cells, and $p$-value = 0.224 for pooled time points of % Ki-67$^{hi}$ Tet$^+$ versus $T_N$ cells; for MCMV$^{ie2SL}$, $p$-value = 0.583 for pooled time points of % Ki-67$^{hi}$ Tet$^+$ versus $T_{EM}$ cells, $p$-value > 0.999 for pooled time points of % Ki-67$^{hi}$ Tet$^+$ versus $T_{CM}$ cells, and $p$-value = 0.389 for pooled time points of % Ki-67$^{hi}$ Tet$^+$ versus $T_N$ cells; for MCMV$^{m45SL}$, $p$-value = 0.938 for pooled time points of % Ki-67$^{hi}$ Tet$^+$ versus $T_{EM}$ cells, $p$-value > 0.999 for pooled time points of % Ki-67$^{hi}$ Tet$^+$ versus $T_{CM}$ cells, and $p$-value = 0.088 for pooled time points of % Ki-67$^{hi}$ Tet$^+$ versus $T_N$ cells. Pooled samples of different time points were compared using Kruskal–Wallis and Dunn's multiple comparison tests. Data are pooled from two independent experiments. Bars represent median percentages.

cell proliferation, we next studied the average production and loss rates of the cells using in vivo deuterium labeling.

### *Kinetics of $T_N$, $T_{CM}$, and $T_{EM}$ CD8$^+$ cells during chronic MCMV infection*

The in vivo kinetics of memory CD8$^+$ T cells have primarily been studied in bulk memory phenotype T cells (5). Here, we quantified the dynamics of $T_N$, $T_{CM}$, $T_{EM}$ and $T_M$ CD8$^+$ cell subsets in chronically infected and uninfected 129/Sv mice. Mice received $^2H_2O$ for 4 wk and were sacrificed at different time points during the labeling and the de-labeling period. We subsequently used previously published mathematical models (5) (see *Materials and Methods*) to quantify the average production and loss rates of $T_N$, $T_{CM}$, $T_{EM}$, and $T_M$ CD8$^+$ cells based on their deuterium labeling data.

Deuterium enrichment curves of $T_N$, $T_{CM}$, $T_{EM}$, and $T_M$ cells were very similar in MCMV$^{ie2SL}$-, MCMV$^{ie2KNL}$-, and MCMV$^{m45SL}$-infected animals (Fig. 3). In line with this, the best fits of the model to the data yielded similar estimates for the average production rates $p$ and the average loss rates of labeled cells $d$* within the $T_N$, $T_{CM}$, $T_{EM}$, and $T_M$ CD8$^+$ cell populations for the three different viruses (Fig. 4A, Table I). The estimated average production rate $p$ of $T_N$ cells during chronic MCMV infection was 0.0090 per day for MCMV$^{ie2SL}$, 0.0095 per day for MCMV$^{ie2KNL}$, and 0.0077 per day for MCMV$^{m45SL}$, suggesting that $T_N$ cells turn over relatively little. In contrast, $T_{CM}$ cells turned over significantly, with average production rates of 0.0132 per day for MCMV$^{ie2SL}$, 0.0151 per day for MCMV$^{ie2KNL}$, and 0.0139 per day for MCMV$^{m45SL}$. The average production rates of $T_{EM}$ cells were consistently the highest, with 0.0204 per day for MCMV$^{ie2SL}$, 0.0229 per day for MCMV$^{ie2KNL}$, and 0.0205 per day for MCMV$^{m45SL}$ (Table I).

### *The turnover rate of MCMV-specific CD8$^+$ T cells is independent of the magnitude of the inflationary response*

To investigate how the size of an MCMV-specific memory T cell response is related to its turnover (20), we quantified the turnover rates of Tet$^+$ CD8$^+$ T cells composing large (MCMV$^{ie2SL}$) and intermediate (MCMV$^{ie2KNL}$) inflationary responses, as well as a low inflationary response (MCMV$^{m45SL}$). Despite the clear differences in the height of the Ag-specific responses induced by these three viruses, the corresponding deuterium enrichment curves of Tet$^+$ CD8$^+$ T cells were very similar (Fig. 3). The best fits of the model to the deuterium-enrichment data of SL Tet$^+$ CD8$^+$ T cells in MCMV$^{ie2SL}$- and MCMV$^{m45SL}$-infected mice (Fig. 3) confirmed that,

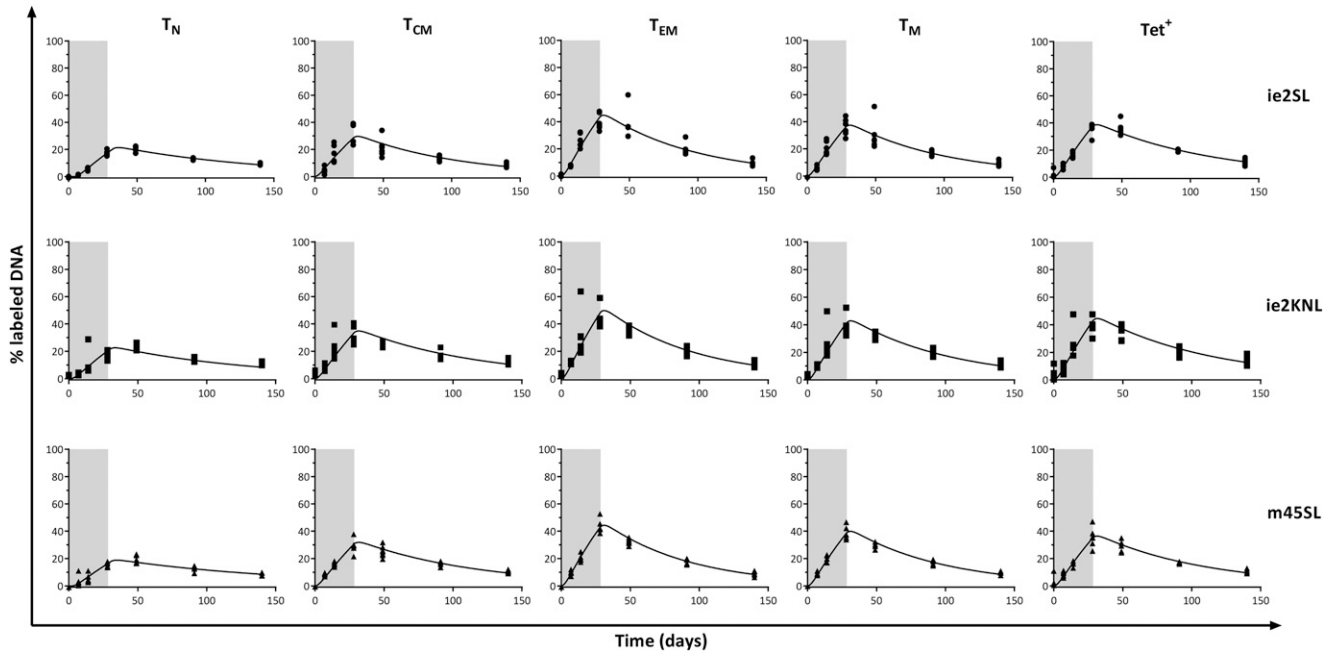


**FIGURE 3.** Deuterium labeling of tetramer-negative and $Tet^+$ $CD8^+$ T cells in MCMV-infected mice. Deuterium enrichment in the DNA of $T_N$, $T_{CM}$, $T_{EM}$, and $T_M$ cells and $Tet^+$ $CD8^+$ T cells 120 d after $MCMV^{ie2SL}$, $MCMV^{ie2KNL}$, or $MCMV^{m45SL}$ infection. The curves represent the best fits of the model (5) to the deuterium enrichment data. Label enrichment was scaled between 0 and 100% by dividing all enrichment levels by the estimated maximum enrichment level of thymocytes (Supplemental Fig. 2, Supplemental Table I). Parameter estimates corresponding to the best fits are given in Table I.

despite the 3-fold difference in the size of these inflationary responses (Fig. 1A) and their different $T_{CM}$ and $T_{EM}$ compositions (Fig. 1B), their average production rates $p$ and loss rates of labeled cells $d^*$ were not significantly different (Fig. 4A, Table I). We estimated that SL $Tet^+$ $CD8^+$ T cells had an average production rate of 0.0169 per day in $MCMV^{ie2SL}$-infected mice and 0.0161 per day in $MCMV^{m45SL}$-infected mice. For KNL-specific T cells, which comprised the intermediate inflationary response, we found an average production rate of 0.0195 per day (Table I). Thus, there were no substantial differences in the average turnover rates of $Tet^+$ $CD8^+$ T cells composing large, intermediate, and low inflationary responses.

### *MCMV-specific $CD8^+$ T cells do not have significantly longer lifespans than do memory phenotype $CD8^+$ T cells*

Finally, to investigate the hypothesis that accumulation of inflationary responses in MCMV is due to accumulation of long-lived cells, we compared the average turnover rates of MCMV-specific ($Tet^+$) $CD8^+$ T cells to those of tetramer-negative $T_M$ $CD8^+$ cells (see *Materials and Methods*). When comparing the best fits of the individual datasets, we found no statistical indication that $T_M$ cells and $Tet^+$ T cells had different production rates $p$ or loss rates of labeled cells $d^*$ (Fig. 4A, Table I).

Since the average loss rate $d^*$ of labeled cells may not be representative of the cell population as a whole (24), we used additional information on absolute cell numbers to compare the average loss rates $d$ of $Tet^+$ and $T_M$ cells. Although these absolute cell numbers are notoriously noisy, we estimated a slight increase in cell numbers in the $T_{CM}$, $T_{EM}$, $T_M$, and $Tet^+$ $CD8^+$ T cell populations (Table II, Supplemental Fig. 3). The average production rates $p$ may thus not be equal to the average loss rates $d$ of cells. Even when accounting for this rate of increase, $r$, in cell numbers, we found very similar average loss rates $d$ (where $d = p - r$, see *Materials and Methods*)

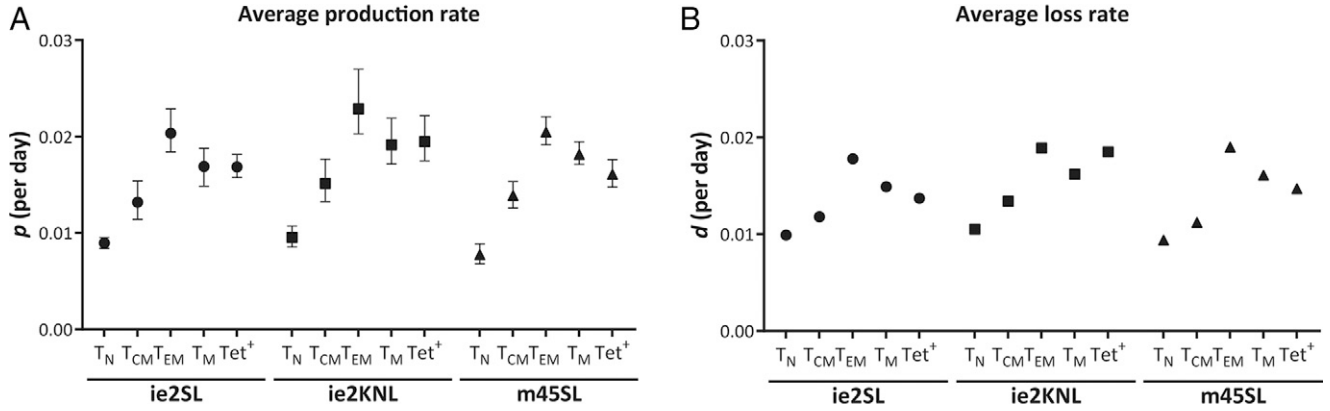


**FIGURE 4.** Average production and loss rates of T cells in MCMV-infected mice. (**A** and **B**) Estimated average production rates $p$ per day (A) and average loss rates $d$ per day (B) for $T_N$, $T_{CM}$, $T_{EM}$ and $T_M$ $CD8^+$ T cells and $Tet^+$ memory $CD8^+$ T cells. (A) Average production rates ($p$) were based on the best fits of the deuterium labeling data of Fig. 3. Their values are reported in Table I. Whiskers represent the corresponding 95% confidence intervals. (B) The average loss rates ($d$) were calculated from $d = p - r$, using the best estimates of $p$ (Table I) and the estimated growth rate ($r$) of the specific T cell population (Table II). Because the average loss rates were calculated based on other parameters, they are given without 95% confidence intervals.

Table I. Average production rates and loss rates of labeled cells in MCMV-infected mice

| CD8$^+$ T Cell Subset | MCMV$^{ie2SL}$ | MCMV$^{ie2KNL}$ | MCMV$^{m45SL}$ |
|---|---|---|---|
| Average production rate per day ($p$) | | | |
| $T_N$ | 0.0090 (0.0084; 0.0095) | 0.0095 (0.0085; 0.0107) | 0.0077 (0.0068; 0.0089) |
| $T_{CM}$ | 0.0132 (0.0114; 0.0154) | 0.0151 (0.0133; 0.0177) | 0.0139 (0.0126; 0.0153) |
| $T_{EM}$ | 0.0204 (0.0184; 0.0229) | 0.0229 (0.0203; 0.0270) | 0.0205 (0.0192; 0.0221) |
| $T_M$ | 0.0169 (0.0149; 0.0188) | 0.0192 (0.0172; 0.0219) | 0.0182 (0.0171; 0.0195) |
| Tet$^+$ | 0.0169 (0.0158; 0.0182) | 0.0195 (0.0175; 0.0222) | 0.0161 (0.0147; 0.0176) |
| Average loss rate of labeled cells per day ($d$*) | | | |
| $T_N$ | 0.0090 (0.0084; 0.0095) | 0.0095 (0.0085; 0.0107) | 0.0077 (0.0068; 0.0089) |
| $T_{CM}$ | 0.0131 (0.0111; 0.0160) | 0.0113 (0.0093; 0.0142) | 0.0115 (0.0102; 0.0130) |
| $T_{EM}$ | 0.0146 (0.0130; 0.0163) | 0.0153 (0.0134; 0.0180) | 0.0157 (0.0143; 0.0170) |
| $T_M$ | 0.0141 (0.0124; 0.0158) | 0.0135 (0.0118; 0.0160) | 0.0146 (0.0135; 0.0161) |
| Tet$^+$ | 0.0116 (0.0104; 0.0128) | 0.0120 (0.0100; 0.0143) | 0.0126 (0.0113; 0.0140) |

Estimated parameters and their corresponding 95% confidence intervals are shown. For $T_N$ cells, we report the best fits of the model with $p = d$, as allowing for different values of $p$ and $d$ did not significantly improve the fit to the data (for significance, $p$-value of $F$ test = 1 for MCMV$^{ie2SL}$, $p$-value of $F$ test = 0.09 for MCMV$^{ie2KNL}$, and $p$-value of $F$ test = 0.54 for MCMV$^{m45SL}$).

of $T_M$ and Tet$^+$ cells in MCMV$^{ie2SL}$-, MCMV$^{ie2KNL}$-, and MCMV$^{m45SL}$-infected mice (Fig. 4B, Table II). We thus found no evidence for the previously proposed idea that CMV-specific T cells are longer-lived than other memory T cells (20).

Although an advantage of the current study is the face-to-face comparison of Tet$^+$ and tetramer-negative cells in the same mouse, it is more than likely that the tetramer-negative T cell populations still contained MCMV-specific CD8$^+$ T cells specific for other MCMV epitopes (17, 18, 21). We wondered whether this could have masked possible differences in the turnover of MCMV-specific and non–MCMV-specific memory CD8$^+$ T cells. To investigate this, we compared the deuterium enrichment levels of $T_N$, $T_{CM}$, $T_{EM}$, and $T_M$ cells in MCMV-infected mice to those in uninfected mice. Because these levels were very similar (Supplemental Fig. 4), we conclude that the expected lifespan of MCMV-specific memory CD8$^+$ T cells is not significantly different from that of other memory-phenotype CD8$^+$ T cells.

## Discussion

During the chronic phase of MCMV infection, we found no evidence that MCMV-specific CD8$^+$ T cells are longer-lived or produced at higher rates than do bulk memory-phenotype CD8$^+$ T cells. These findings are in line with our recent findings in humans, which showed that CMV-specific CD8$^+$ T cells had similar turnover rates as bulk memory CD8$^+$ T cells (28). Both outcomes are remarkable in the light of a previously published deuterated-glucose labeling study in humans, which reported that CMV-specific CD8$^+$ T cells incorporated less deuterium than did CD45RO$^+$ (memory) T cells (20), which led to the hypothesis that inflating responses are composed of relatively long-lived memory T cells. We found that the turnover rates of Ag-specific T cells composing inflationary responses that varied up to 3-fold in size were not significantly different. This adds further support to our conclusion that the magnitude of inflationary responses is not explained by extended lifespans of MCMV-specific T cells.

To interpret the deuterium labeling data, we used a previously proposed kinetic heterogeneity model (24), which yields the average production rate $p$ of cells, as well the average loss rate $d$* of labeled cells. It was previously explained that cell populations in steady state typically yield $d^* > p$, because $p$ is representative of all cells in the population, whereas $d$* is biased toward cells that have just divided (24). The estimated value of $p$ can thus safely be interpreted as the average production rate of cells, which apparently does not differ between inflationary CMV-specific T cell responses and bulk memory T cells. The cellular production that we measured by in vivo deuterium labeling captures both T cell division as well as a possible influx of cells from the naive compartment. Although it has previously been shown that naive T cells can continuously be recruited into the MCMV-specific T cell response (19), the contribution of this influx is probably relatively small, as memory inflation in mice was shown to be hardly affected by thymectomy (29, 30). Thus, assuming that the vast majority of MCMV-specific cells are formed by peripheral T cell division, and not by continuous recruitment of new naive MCMV-specific T cells into the memory

Table II. Average population growth rates and average loss rates in MCMV-infected mice

| CD8$^+$ T Cell Subset | MCMV$^{ie2SL}$ | MCMV$^{ie2KNL}$ | MCMV$^{m45SL}$ |
|---|---|---|---|
| Average growth/decay rate of the cell population per day ($r$) | | | |
| $T_N$ | −0.00093 (−0.0028; 0.00015) | −0.00094 (−0.0039; 0.00065) | −0.0016 (−0.004; −0.0004) |
| $T_{CM}$ | 0.0014 (0.00032; 0.0024) | 0.0017 (−0.0028; 0.0027) | 0.0027 (0.0007; 0.0044) |
| $T_{EM}$ | 0.0026 (0.0013; 0.0037) | 0.0040 (0.00025; 0.0068) | 0.0015 (0.00014; 0.0028) |
| $T_M$ | 0.0020 (0.000895; 0.0029) | 0.0030 (−0.00033; 0.0043) | 0.0021 (0.00083; 0.0033) |
| Tet$^+$ | 0.0032 (0.0021; 0.0045) | 0.001 (−0.0021; 0.008) | 0.0014 (−0.00025; 0.0029) |
| Calculated average T cell loss rate per day ($d$) | | | |
| $T_N$ | 0.0099 | 0.0105 | 0.00939 |
| $T_{CM}$ | 0.0118 | 0.0134 | 0.0112 |
| $T_{EM}$ | 0.0178 | 0.0189 | 0.0190 |
| $T_M$ | 0.0149 | 0.0162 | 0.0161 |
| Tet$^+$ | 0.0137 | 0.0185 | 0.0147 |

T cell loss rates ($d$) were calculated using the estimated average production rates ($p$) (from the deuterium labeling experiments, Table I) and the estimated overall growth/decay rates ($r$) of the specific T cell populations (followed for 550 days, Supplemental Fig. 3) (see *Materials and Methods*). Overall growth/decay rates of the specific T cell populations were estimated by simultaneously estimating each population size at the start of the experiment (i.e., 120 dpi), N(0), of which the values are given in Supplemental Table I. Estimated growth rates are reported with their corresponding 95% confidence intervals in brackets. Because the average loss rates were calculated based on other parameters, they are given without 95% confidence intervals.

pool, the similar production rates of $Tet^+$ and $T_M$ cells imply that MCMV-specific T cells do not divide more frequently than do other memory T cells, which is supported by their similar Ki-67 expression levels. It has recently been shown that the MCMV-specific inflationary T cell response is "fueled" by a subset of $Tcf1^+$ MCMV-specific T cells (31), and that continual, stochastic encounters with MCMV maintain the inflationary response (32).

To compare the average loss rates of $Tet^+$ and $T_M$ cells, we used additional information on absolute cell numbers, which confirmed that also the expected lifespans of $Tet^+$ and $T_M$ cells are very similar. We found that the expected lifespan (calculated as $1/d$) of bulk memory-phenotype T cells was ~65 days, whereas that of MCMV-specific T cells was 73 days for the large inflationary response in $MCMV^{ie2SL}$-infected mice, 54 days for the intermediate inflationary response in $MCMV^{ie2KNL}$-infected mice, and 68 days for the low inflationary response in $MCMV^{m45SL}$-infected mice. These estimates are well in line with previous studies showing the dynamic behavior of inflating responses (19). We thus found no evidence for the previously proposed idea that CMV-specific T cells are longer-lived than other memory T cells (20). Instead, our data suggest that the explanation for the size differences between MCMV-specific $CD8^+$ T cell responses and for memory inflation in general should be sought earlier during infection. In line with this, several studies have shown that the inflationary potential of CMV-specific T cells is set early, during the acute phase of the response (19, 30), and is linked to the number of primed KLRG1- CMV-specific $CD8^+$ T cells (33) and to the early transcriptomic profile and $T_{CM}$ cell precursor content of the CMV-specific $CD8^+$ T cells (34).

Nonsteady cell numbers in some of the populations may explain why we sometimes found values of $d^*$ lower than $p$ (see Table I). This is typically not observed in deuterium labeling experiments (24), and it suggests that cells that have recently divided live longer than other cells in the population. Alternatively, for populations that are not in steady state, if cellular turnover is dependent on cell densities, average production rates may decrease during the labeling experiment, although cell numbers are increasing. This could explain why, contrary to what is typically observed for populations in steady state, some turnover rates during the de-labeling phase were lower than during the up-labeling phase (A.C. Swain, J. Drylewicz, J.A.M. Borghans, and R.J. de Boer, manuscript in preparation). In this light, it is interesting to note that the T cell repertoire against CMV has recently been shown to continuously evolve during chronic infection, in that the relative immunodominance of high-affinity clones declines during chronic infection, most likely due to cellular senescence (35).

A previous study in humans reported that YFV-specific $CD8^+$ T cells triggered upon YFV vaccination divide sporadically, approximately every 666 days (11), and less than bulk memory T cells. It was argued that the shorter intermitotic times of bulk memory T cells probably reflect their continuous Ag stimulation (11). In line with this hypothesis, we found that MCMV-specific $CD8^+$ T cells, which are repeatedly exposed to their cognate Ag, have similar lifespans as bulk memory-phenotype $CD8^+$ T cells, which may also be continuously exposed to commensal and environmental Ags. However, the observation that lymphocytic choriomeningitis virus–specific memory $CD8^+$ T cells transferred into naive mice had similar turnover rates to those of bulk memory-phenotype $CD8^+$ T cells (36) suggests that even Ag-specific T cells maintained in the absence of cognate Ag can turnover as fast as bulk memory-phenotype T cells. Although we cannot exclude the possibility that the differences in the maintenance of YFV-, MCMV-, and lymphocytic choriomeningitis virus–specific memory $CD8^+$ T cells are due to mouse and human differences, the characteristics of different Ag-specific memory T cells may also depend on the nature of the infection, the duration of the stimulus, and the concomitant response to other Ags. It is therefore perhaps not surprising that Ag-specific T cell responses against different infections have different dynamics (37). Future studies into the dynamics of memory T cells specific for Ags that are presented persistently (chronic), intermittently (latent reactivating), or only once (acute) are needed to gain more insight into how Ag-specific memory T cell responses are maintained in mice and humans.

Chronic CMV infection in both mice and humans is under constant immune surveillance and triggers ongoing $CD8^+$ T cell responses. It is thought that CMV infection modulates the peripheral lymphoid pool (38, 39) and affects T cell differentiation and function (40), not only of CMV-specific T cells but also of T cells with other specificities (41). Under this hypothesis, we directly compared the dynamics of $T_N$, $T_{CM}$, $T_{EM}$, and $T_M$ cells in uninfected and chronically MCMV-infected mice (Supplemental Fig. 4) and found no significant differences in their kinetics. Despite differences in the composition of the T cell pool, our results therefore suggest that the dynamics of non–MCMV-specific $CD8^+$ T cells are not substantially affected during chronic MCMV infection. We previously observed that also cellular immune function was maintained during latency, as responses to heterologous virus infection and immune protection were not diminished in mice latently infected with MCMV or other herpesviruses (42).

The large prevalence of chronic CMV infection in the human population (>50%) (43) and its effect on healthy aging (44–46), together with the emerging interest in CMV-based vector vaccines (15), highlight the need to understand how CMV-specific $CD8^+$ T cell responses are maintained. In vivo MCMV infection provided us with the means to address fundamental questions about the maintenance and turnover of inflated $CD8^+$ T cell responses. The finding that the maintenance of inflationary MCMV-specific $CD8^+$ T cells does not differ from that of low inflationary memory $CD8^+$ T cells suggests that inflationary $CD8^+$ T cell responses, such as those induced by CMV-based vector vaccines, may also result in a memory $CD8^+$ T cell response of high magnitude without substantial alterations in the dynamics of the cells.

## Acknowledgments

We thank Ramon Arens for generously providing all MHC-peptide tetramers, Nienke Vrisekoop for help and support with the animal experiments, Derek Macallan and Linda Hadcocks for measuring $^2H_2O$ enrichment in the body water of the uninfected mice, and Janine Schreiber and Lothar Gröbe for technical assistance.

## Disclosures

The authors have no financial conflicts of interest.

## References

1. Michie, C. A., A. McLean, C. Alcock, and P. C. L. Beverley. 1992. Lifespan of human lymphocyte subsets defined by CD45 isoforms. *Nature* 360: 264–265.
2. Crotty, S., and R. Ahmed. 2004. Immunological memory in humans. *Semin. Immunol.* 16: 197–203.
3. Vrisekoop, N., I. den Braber, A. B. de Boer, A. F. C. Ruiter, M. T. Ackermans, S. N. van der Crabben, E. H. R. Schrijver, G. Spierenburg, H. P. Sauerwein, M. D. Hazenberg, et al. 2008. Sparse production but preferential incorporation of recently produced naive T cells in the human peripheral pool. *Proc. Natl. Acad. Sci. USA* 105: 6115–6120.
4. Macallan, D. C., B. Asquith, A. J. Irvine, D. L. Wallace, A. Worth, H. Ghattas, Y. Zhang, G. E. Griffin, D. F. Tough, and P. C. Beverley. 2003. Measurement and modeling of human T cell kinetics. *Eur. J. Immunol.* 33: 2316–2326.
5. Westera, L., J. Drylewicz, I. den Braber, T. Mugwagwa, I. van der Maas, L. Kwast, T. Volman, E. H. R. van de Weg-Schrijver, I. Bartha, G. Spierenburg, et al. 2013. Closing the gap between T-cell life span estimates from stable isotope-labeling studies in mice and humans. *Blood* 122: 2205–2212.

6. Wallace, D. L., Y. Zhang, H. Ghattas, A. Worth, A. Irvine, A. R. Bennett, G. E. Griffin, P. C. L. Beverley, D. F. Tough, and D. C. Macallan. 2004. Direct measurement of T cell subset kinetics in vivo in elderly men and women. *J. Immunol.* 173: 1787–1794.
7. Hellerstein, M. K., R. A. Hoh, M. B. Hanley, D. Cesar, D. Lee, R. A. Neese, and J. M. McCune. 2003. Subpopulations of long-lived and short-lived T cells in advanced HIV-1 infection. *J. Clin. Invest.* 112: 956–966.
8. Borghans, J. A. M., K. Tesselaar, and R. J. de Boer. 2018. Current best estimates for the average lifespans of mouse and human leukocytes: reviewing two decades of deuterium-labeling experiments. *Immunol. Rev.* 285: 233–248.
9. Macallan, D. C., J. A. Borghans, and B. Asquith. 2017. Human T cell memory: a dynamic view. *Vaccines (Basel)* 5: 5.
10. Macallan, D. C., D. Wallace, Y. Zhang, C. De Lara, A. T. Worth, H. Ghattas, G. E. Griffin, P. C. L. Beverley, and D. F. Tough. 2004. Rapid turnover of effector-memory CD4$^+$ T cells in healthy humans. *J. Exp. Med.* 200: 255–260.
11. Akondy, R. S., M. Fitch, S. Edupuganti, S. Yang, H. T. Kissick, K. W. Li, B. A. Youngblood, H. A. Abdelsamed, D. J. McGuire, K. W. Cohen, et al. 2017. Origin and differentiation of human memory CD8 T cells after vaccination. *Nature* 552: 362–367.
12. O'Hara, G. A., S. P. M. Welten, P. Klenerman, and R. Arens. 2012. Memory T cell inflation: understanding cause and effect. *Trends Immunol.* 33: 84–90.
13. Kim, J., A.-R. Kim, and E.-C. Shin. 2015. Cytomegalovirus infection and memory T cell inflation. *Immune Netw.* 15: 186–190.
14. Klenerman, P., and A. Oxenius. 2016. T cell responses to cytomegalovirus. *Nat. Rev. Immunol.* 16: 367–377.
15. Bolinger, B., S. Sims, L. Swadling, G. O'Hara, C. de Lara, D. Baban, N. Saghal, L. N. Lee, E. Marchi, M. Davis, et al. 2015. Adenoviral vector vaccination induces a conserved program of CD8$^+$ T cell memory differentiation in mouse and man. *Cell Rep.* 13: 1578–1588.
16. Karrer, U., S. Sierro, M. Wagner, A. Oxenius, H. Hengel, U. H. Koszinowski, R. E. Phillips, and P. Klenerman. 2003. Memory inflation: continuous accumulation of antiviral CD8$^+$ T cells over time. *J. Immunol.* 170: 2022–2029.
17. Munks, M. W., K. S. Cho, A. K. Pinto, S. Sierro, P. Klenerman, and A. B. Hill. 2006. Four distinct patterns of memory CD8 T cell responses to chronic murine cytomegalovirus infection. *J. Immunol.* 177: 450–458.
18. Dekhtiarenko, I., M. A. Jarvis, Z. Ruzsics, and L. Čičin-Šain. 2013. The context of gene expression defines the immunodominance hierarchy of cytomegalovirus antigens. *J. Immunol.* 190: 3399–3409.
19. Snyder, C. M., K. S. Cho, E. L. Bonnett, S. van Dommelen, G. R. Shellam, and A. B. Hill. 2008. Memory inflation during chronic viral infection is maintained by continuous production of short-lived, functional T cells. *Immunity* 29: 650–659.
20. Wallace, D. L., J. E. Masters, C. M. De Lara, S. M. Henson, A. Worth, Y. Zhang, S. R. Kumar, P. C. Beverley, A. N. Akbar, and D. C. Macallan. 2011. Human cytomegalovirus-specific CD8$^+$ T-cell expansions contain long-lived cells that retain functional capacity in both young and elderly subjects. *Immunology* 132: 27–38.
21. Borkner, L., K. M. Sitnik, I. Dekhtiarenko, A.-K. Pulm, R. Tao, I. Drexler, and L. Cicin-Sain. 2017. Immune protection by a cytomegalovirus vaccine vector expressing a single low-avidity epitope. *J. Immunol.* 199: 1737–1747.
22. Oduro, J. D., A. Redeker, N. A. W. Lemmermann, L. Ebermann, T. F. Marandu, I. Dekhtiarenko, J. K. Holzki, D. H. Busch, R. Arens, and L. Čičin-Šain. 2016. Murine cytomegalovirus (CMV) infection via the intranasal route offers a robust model of immunity upon mucosal CMV infection. *J. Gen. Virol.* 97: 185–195.
23. Westera, L., V. van Hoeven, J. Drylewicz, G. Spierenburg, J. F. van Velzen, R. J. de Boer, K. Tesselaar, and J. A. Borghans. 2015. Lymphocyte maintenance during healthy aging requires no substantial alterations in cellular turnover. *Aging Cell* 14: 219–227.
24. Asquith, B., C. Debacq, D. C. Macallan, L. Willems, and C. R. M. Bangham. 2002. Lymphocyte kinetics: the interpretation of labelling data. *Trends Immunol.* 23: 596–601.
25. Soetaert, K., T. Petzoldt, and R. W. Setzer. 2010. Solving differential equations in R: package deSolve. *J. Stat. Softw.* 33: 1–25.
26. Mitrović, M., J. Arapović, S. Jordan, N. Fodil-Cornu, S. Ebert, S. M. Vidal, A. Krmpotić, M. J. Reddehase, and S. Jonjić. 2012. The NK cell response to mouse cytomegalovirus infection affects the level and kinetics of the early CD8$^+$ T-cell response. *J. Virol.* 86: 2165–2175.
27. Sun, Y., K. Yang, T. Bridal, and A. G. Ehrhardt. 2016. Robust Ki67 detection in human blood by flow cytometry for clinical studies. *Bioanalysis* 8: 2399–2413.
28. van den Berg, S. P. H., L. Y. Derksen, J. Drylewicz, N. M. Nanlohy, L. Beckers, J. Lanfermeijer, S. N. Gessel, M. Vos, S. A. Otto, R. J. de Boer, et al. 2021. Quantification of T-cell dynamics during latent cytomegalovirus infection in humans. *PLoS Pathog.* DOI: 10.1371/journal.ppat.1010152.
29. Loewendorf, A. I., R. Arens, J. F. Purton, C. D. Surh, and C. A. Benedict. 2011. Dissecting the requirements for maintenance of the CMV-specific memory T-cell pool. *Viral Immunol.* 24: 351–355.
30. Welten, S. P. M., N. S. Baumann, and A. Oxenius. 2019. Fuel and brake of memory T cell inflation. *Med. Microbiol. Immunol. (Berl.)* 208: 329–338.
31. Welten, S. P. M., A. Yermanos, N. S. Baumann, F. Wagen, N. Oetiker, I. Sandu, A. Pedrioli, J. D. Oduro, S. T. Reddy, L. Cicin-Sain, et al. 2020. Tcf1$^+$ cells are required to maintain the inflationary T cell pool upon MCMV infection. *Nat. Commun.* 11: 2295.
32. Smith, C. J., V. Venturi, M. F. Quigley, H. Turula, E. Gostick, K. Ladell, B. J. Hill, D. Himelfarb, K. M. Quinn, H. Y. Greenaway, et al. 2020. Stochastic expansions maintain the clonal stability of CD8$^+$ T cell populations undergoing memory inflation driven by murine cytomegalovirus. *J. Immunol.* 204: 112–121.
33. Baumann, N. S., S. P. M. Welten, N. Torti, K. Pallmer, M. Borsa, I. Barnstorf, J. D. Oduro, L. Cicin-Sain, and A. Oxenius. 2019. Early primed KLRG1$^-$ CMV-specific T cells determine the size of the inflationary T cell pool. *PLoS Pathog.* 15: e1007785.
34. Grassmann, S., L. Mihatsch, J. Mir, A. Kazeroonian, R. Rahimi, S. Flommersfeld, K. Schober, I. Hensel, J. Leube, L. O. Pachmayr, et al. 2020. Early emergence of T central memory precursors programs clonal dominance during chronic viral infection. *Nat. Immunol.* 21: 1563–1573.
35. Schober, K., F. Voit, S. Grassmann, T. R. Müller, J. Eggert, S. Jarosch, B. Weißbrich, P. Hoffmann, L. Borkner, E. Nio, et al. 2020. Reverse TCR repertoire evolution toward dominant low-affinity clones during chronic CMV infection. *Nat. Immunol.* 21: 434–441.
36. Choo, D. K., K. Murali-Krishna, R. Anita, and R. Ahmed. 2010. Homeostatic turnover of virus-specific memory CD8 T cells occurs stochastically and is independent of CD4 T cell help. *J. Immunol.* 185: 3436–3444.
37. Althaus, C. L., V. V. Ganusov, and R. J. De Boer. 2007. Dynamics of CD8$^+$ T cell responses during acute and chronic lymphocytic choriomeningitis virus infection. *J. Immunol.* 179: 2944–2951.
38. Chidrawar, S., N. Khan, W. Wei, A. McLarnon, N. Smith, L. Nayak, and P. Moss. 2009. Cytomegalovirus-seropositivity has a profound influence on the magnitude of major lymphoid subsets within healthy individuals. *Clin. Exp. Immunol.* 155: 423–432.
39. Derhovanessian, E., A. Larbi, and G. Pawelec. 2009. Biomarkers of human immunosenescence: impact of cytomegalovirus infection. *Curr. Opin. Immunol.* 21: 440–445.
40. Miles, D. J. C., M. Sanneh, B. Holder, S. Crozier, S. Nyamweya, E. S. Touray, M. S. Palmero, S. M. A. Zaman, S. Rowland-Jones, M. van der Sande, and H. Whittle. 2008. Cytomegalovirus infection induces T-cell differentiation without impairing antigen-specific responses in Gambian infants. *Immunology* 124: 388–400.
41. Lanfermeijer, J., P. C. de Greef, M. Hendriks, M. Vos, J. van Beek, J. A. M. Borghans, and D. van Baarle. 2021. Age and CMV-infection jointly affect the EBV-specific CD8$^+$ T-cell repertoire. *Front. Aging* 2. Available at: https://doi.org/10.3389/fragi.2021.665637.
42. Marandu, T. F., J. D. Oduro, L. Borkner, I. Dekhtiarenko, J. L. Uhrlaub, A. Drabig, A. Kröger, J. Nikolich-Zugich, and L. Cicin-Sain. 2015. Immune protection against virus challenge in aging mice is not affected by latent herpesviral infections. *J. Virol.* 89: 11715–11717.
43. Cannon, M. J., D. S. Schmid, and T. B. Hyde. 2010. Review of cytomegalovirus seroprevalence and demographic characteristics associated with infection. *Rev. Med. Virol.* 20: 202–213.
44. Brodin, P., V. Jojic, T. Gao, S. Bhattacharya, C. J. L. Angel, D. Furman, S. Shen-Orr, C. L. Dekker, G. E. Swan, A. J. Butte, et al. 2015. Variation in the human immune system is largely driven by non-heritable influences. *Cell* 160: 37–47.
45. Roberts, E. T., M. N. Haan, J. B. Dowd, and A. E. Aiello. 2010. Cytomegalovirus antibody levels, inflammation, and mortality among elderly Latinos over 9 years of follow-up. *Am. J. Epidemiol.* 172: 363–371.
46. Aiello, A. E., Y.-L. Chiu, and D. Frasca. 2017. How does cytomegalovirus factor into diseases of aging and vaccine responses, and by what mechanisms?*Geroscience* 39: 261–271.